

Multiplex Immuno-MALDI-TOF MS for Targeted Quantification of Protein Biomarkers and Their Proteoforms Related to Inflammation and Renal Dysfunction

Jie Gao,^{*,†} Klaus Meyer,[§] Katrin Borucki,^{||} and Per Magne Ueland^{†,‡}

[†]Department of Clinical Science, University of Bergen, 5021 Bergen, Norway

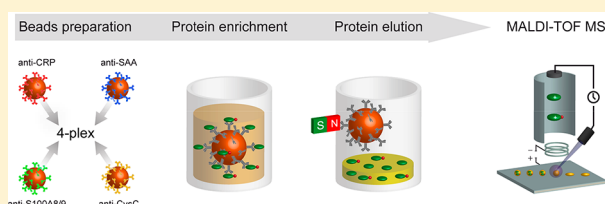
[‡]Laboratory of Clinical Biochemistry, Haukeland University Hospital, 5021 Bergen, Norway

[§]Bevital AS, Jonas Lies veg 87, Laboratory Building, Ninth Floor, 5021 Bergen, Norway

^{||}Institute for Clinical Chemistry and Pathobiochemistry, Otto-von-Guericke University Magdeburg, Leipziger Strasse 44, 39120 Magdeburg, Germany

Supporting Information

ABSTRACT: Circulating proteins are widely used as biomarkers in clinical applications for the diagnosis, prediction, and treatment of numerous diseases. Immunoassays are the most common technologies for quantification of protein biomarkers and exist in various formats. Traditional immunoassays offer sensitive and fast analyses but cannot differentiate between proteoforms. Protein microheterogeneity, mainly due to post-translational modification, has been recognized as a fingerprint for different pathologies, and knowledge about proteoforms is an important step toward personalized medicine. Mass spectrometry (MS) has emerged to be a powerful technique for the characterization and quantification of proteoforms. We have established a novel four-plex immunoassay based on Matrix-Assisted Laser Desorption/Ionization Time-Of-Flight (MALDI-TOF) MS for the targeted quantification of the inflammatory markers C-reactive protein (CRP), serum amyloid A (SAA), and calprotectin (S100A8/9) and the kidney function marker cystatin C (CysC). Antibodies were covalently bound to superparamagnetic beads, which delivered robust and fast sample processing. Polyhistidine-tagged recombinant target proteins were used as internal standards for quantification. Our method identified a number of proteoforms for SAA ($n = 11$), S100A8/9 ($n = 4$) and CysC ($n = 4$). The assay was characterized by low limits of detection (0.01–0.06 $\mu\text{g}/\text{mL}$) and low coefficients of variation (3.8–9.4%). Method validation demonstrated good between-assay agreement with immuno-turbidimetry ($R^2 = 0.963$ for CRP), ELISA ($R^2 = 0.958$ for SAA; $R^2 = 0.913$ for S100A8/9), and nephelometry ($R^2 = 0.963$ for CysC). The low sample consumption of 20 μL and the high sample throughput of 384 samples per day make this targeted immuno-MALDI approach suited for assessment of inflammatory and renal status in large cohort studies based on precious biobanks samples.



Protein biomarkers have attracted increasing attention during the past few years for the diagnosis, risk assessment, and therapy of diseases.^{1,2} Microheterogeneity increases the diversity of protein biomarkers, as mutations, alternative splicing, or post-translational modifications (PTMs) result in proteoforms, which can play different roles in biological processes and may vary between pathologies and individuals.^{3,4}

Knowledge about protein heterogeneity is a key to personalized diagnostics and treatment of disease. Thus, there is increasing demand for quantitative techniques for investigation of biomarker diversity. Discrimination of proteoforms by traditional immunological techniques such as enzyme-linked immunosorbent assay (ELISA) or radioimmunoassay (RIA) is difficult or impossible.^{5,6} They either capture the wild type form only or the antibody cannot discriminate the wild type form from the proteoforms.

Mass spectrometry (MS) allows determination of the molecular mass, differentiation between proteoforms, and multiplexing of biomarkers, which are advantages when

compared to traditional immunoassay. Quantification of peptides and proteins by MS is carried out as bottom-up or top-down approaches.^{7,8} Bottom-up methods identify the proteins indirectly using their constituent peptide fragments, whereas top-down assays detect the intact protein and are superior methods for discrimination of structurally related proteoforms. Matrix-Assisted Desorption/Ionization Time-of-Flight (MALDI-TOF) MS is known to be a sensitive and rapid method for the detection of large biomolecules.^{9,10} When combined with immuno-affinity capture, MALDI-TOF MS has been proven as a powerful tool for the targeted quantification of intact proteins.^{6,11,12} Combination of immuno-affinity with MALDI MS has to overcome two challenges, i.e., design of a robust and compatible assay format for protein capture and application of intact proteins as internal standards (ISs). During

Received: November 30, 2017

Accepted: February 8, 2018

Published: February 8, 2018

the past decade, different formats have been evaluated, which are based on chips,^{13,14} pipetting tips,^{12,15} and magnetic beads (MBs).^{16–18} Especially, the so-called mass spectrometric immunoassay (MSIA) has been applied to various protein biomarkers and has recently become commercially available.¹⁹ Uniformly isotope-labeled proteins and modified recombinant and endogenous proteins have been successfully used as ISs in quantitative analyses.^{11,12,20,21}

Chronic low-grade inflammatory processes have been related to many common diseases including artherosclerosis, diabetes, obesity, rheumatic disorders, and cancer.^{22–26} Many biomarkers of inflammation have been identified. Due to the complexity of inflammatory and immune responses, a combination of multiple markers may perform better in terms of disease prediction, diagnosis, or prognosis than a single marker.

C-reactive protein (CRP) belongs to the pentraxin family of proteins, which is characterized by the calcium-dependent assembly of five monomers forming a radial symmetric ring.²⁷ While the pentameric ring represents the native form in serum and plasma, dissociation results in monomeric CRP (mCRP), which is mostly found in tissues.²⁸ CRP is produced in hepatocytes, mainly under the transcriptional control of cytokines, IL-6 and IL-1. CRP is a major acute-phase reactant and the most important marker for the diagnosis of systemic inflammation in clinical practice. During an acute immune response, levels can increase more than 1000-fold and peak after about 48 h. Low levels of the so-called high-sensitivity (hs-) CRP below 10 $\mu\text{g}/\text{mL}$ are typically found in the general population. Chronically elevated levels within this range have been associated with higher risks of different pathologies, including cardiovascular diseases (CVD), stroke, metabolic syndrome, and cancer.^{29–31}

Serum amyloid A (SAA) is another key acute-phase protein and is coded by four different genes. *SAA1* and *SAA2* encode for the acute-phase proteins, while *SAA3* is an apparent pseudogene and *SAA4* is constitutively expressed.^{32,33} Various single nucleotide polymorphisms have been described for *SAA1* and *SAA2*, and their protein products undergo post-translational truncation, which generates a large number of proteoforms.³⁴ SAA production occurs in the liver and is driven by IL-6, IL-1, and TNF- α . During acute inflammation, SAA is secreted into the circulation where concentrations could increase more than 1000-fold compared to normal values of <5 $\mu\text{g}/\text{mL}$. Increased SAA may become the major lipoprotein of circulating high-density lipoprotein particles (HDL) and thereby may impact cholesterol efflux capacity, suggesting a contribution of high SAA in the pathogenesis of atherosclerosis and CVD.^{35–37} Furthermore, recurrent or persistently high serum SAA concentrations play a key role in the development of secondary or amyloid A (AA) amyloidosis.³⁸ SAA is immunologically highly active, affects several intracellular pathways, and is thought to participate in the pathogenesis of rheumatoid arthritis, obesity, type-2 diabetes, and cancer.^{39–41} As recently shown for type-2 diabetes, disease risk may also be associated with a particular proteoform of SAA.⁴²

Endogenous danger-associated molecular patterns (DAMPs) are intracellular molecules that amplify an immune response and promote inflammation by interaction with Toll-like receptors (TLRs) and receptors for advanced glycation end products (RAGE).⁴³ S100A8 and S100A9 belong to the S100 protein family and are DAMP molecules, which are released from activated or necrotic neutrophils and monocytes/macrophages.⁴⁴ In the presence of Zn^{2+} and Ca^{2+} , they

preferentially form heterocomplexes, also called MRP8/14 or calprotectin (S100A8/9). The exact structure of the calprotectin complex is uncertain and has been described as heterodimer, trimer, or tetramer.^{45–47} Binding of metal ions mediates the complex formation and determines the functional diversity of S100A8/9.^{47–49} S100A9 has been described as three different proteoforms. In diagnostics, S100A8/9 is widely used as a fecal marker for monitoring of inflammatory bowel disease.⁵⁰ Elevated blood levels have been associated with various inflammatory diseases, such as rheumatoid arthritis, atherosclerosis, CVD, metabolic syndrome, and different types of cancer.^{51–54}

Inflammation and chronic kidney disease (CKD) are both linked to pathologies such as CVD, diabetes, and metabolic syndrome.^{55,56} Kidney function is usually monitored by the estimated glomerular filtration rate (eGFR) based on circulating levels of creatinine. Cystatin C (CysC) has become an alternative marker to creatinine, because it is more sensitive to mild kidney dysfunction and less dependent on age, gender, muscle mass, nutritional status, and ethnicity.^{57,58} CysC has a molecular mass of 13 kDa, is a nonglycosylated cysteine protease inhibitor, is produced by all nucleated cells at a constant rate, is freely filtrated by the glomeruli, and is almost completely catabolized in the proximal renal tubules. Tubular secretion of CysC does not occur, and elevated urinary levels have been related to tubular injury.⁵⁹ In addition to CKD, CysC has been related to CVD and different neurological disorders. While higher levels of circulating CysC are associated with increased CVD risk,^{60,61} increased expression and secretion in the brain may have both neurodegenerative as well as neuroprotective effects.^{62,63} Proteoforms of CysC have been identified in blood samples and cerebrospinal fluids^{12,64,65} and may give further insights into pathologies of CKD^{66,67} and neurological disorders.

This work presents a novel immuno-MALDI-TOF MS approach for the simultaneous analyses of CRP, SAA, S100A8/9, and CysC. The method quantifies the markers and their proteoforms in serum/plasma. Immuno-affinity capture is carried out by covalently linked antibodies, immobilized on superparamagnetic beads, which enables flexible assay designs and a quick and easy work flow. Modified recombinant variants of the target proteins serve as internal standards. The fully automated sample preparation requires a low sample volume of 20 μL and makes this method highly suitable for large biobank studies on conditions related to inflammation and renal dysfunction.

EXPERIMENTAL SECTION

Materials. NHS (*N*-hydroxy-succinimide) activated magnetic beads (88827), borate buffer (28341), and TBS-T buffer (28358) were purchased from Thermo Fisher Scientific (Rockford, IL). For collection of the beads, both a magnetic stand for 1.5 mL tubes (MPC-E) from Dynal (Oslo, Norway) and a magnet plate for 96-microtiter plates (Magnum FLX) from Alpaqua (Beverly, MA) were used. Recombinant calprotectin (HC2120) was purchased from HycultBiotech (Uden, Netherlands), polyclonal anti-CRP (235752) from Merck (Darmstadt, Germany), monoclonal anti-SAA (MO-C40028A) from Anogen (Ontario, Canada), monoclonal anti-S100A8/9 (orb108131) from Biorbyt (Cambridge, UK), and polyclonal anti-CysC (PCC2) from Hytest (Turku, Finland). Ultrapure water was produced on a Milli-Q system from Millipore (Billerica, MA). Acetonitrile, trifluoroacetic acid

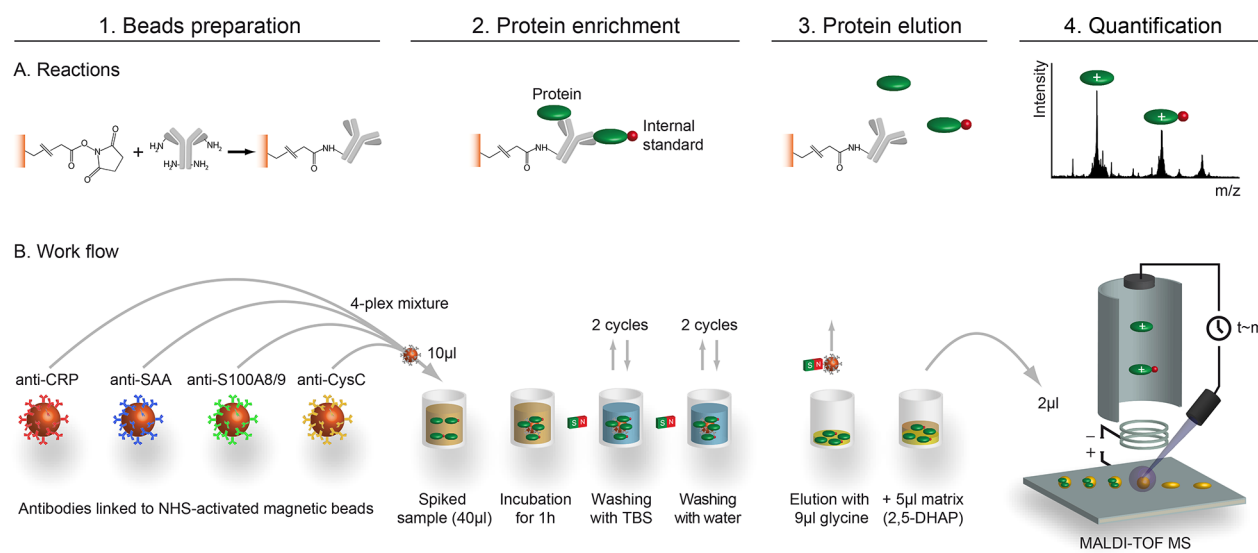


Figure 1. Description of the immuno-MALDI-TOF MS assay. The method consists of four steps starting with preparation of magnetic beads, followed by protein enrichment, protein elution, and finally quantification by MALDI MS. The fundamental reactions (A) and the work flow (B) are illustrated for each step. First, antibodies were linked to superparamagnetic beads by covalent conjugation of the antibody's primary amines with *N*-hydroxysuccinimide (NHS) esters of the functionalized beads. Linking was performed separately for each antibody, which had been diluted to equal concentrations of 0.5 μg/mL. Beads were mixed in equal amounts prior to sample purification. A total of 20 μL of each serum/plasma sample was spiked with 20 μL of internal standard (IS) and was incubated with 10 μL of beads for 1 h, processed in 96-microtiter plates. After protein enrichment, beads were washed two times both with Tris-buffered saline (TBS) and ultrapure water using a 96-well magnet plate for separation of the beads from the liquids. Proteins were released from the antibodies adding 9 μL of 0.1 M glycine solution. Beads were collected by the magnet plate, and the supernatant was transferred into a new microtiter plate. Finally, samples were mixed intensely with 5 μL of 2,5-dihydroxyacetophenone (DHAP) matrix, and 2 μL of the sample/matrix solution was spotted onto an anchor target plate for quantification of the proteoforms by MALDI-TOF MS.

(TFA), 2,5-dihydroxyacetophenone (2,5-DHAP), hydrochloric acid, and ethanolamine were purchased from Sigma (Oslo, Norway). Glycine was from Merck (Darmstadt, Germany). Certified reference sera spiked with CRP (ERM-DA474 IFCC) or CysC (ERM-DA471 IFCC) were obtained from the Reference Materials Unit of the European Commission Joint Research Centre (Geel, Belgium). Certified reference serum (92/680) for SAA was purchased from NIBSC (South Mimms, UK).

Internal Standards. Differently labeled recombinant proteins were used as internal standards. Polyhistidine-tagged recombinant human C-reactive protein (CRP-HIS) was purchased from Acro-Biosystems (Newark, DE; CRP-HS226), serum amyloid A (SAA-HIS) from Biotechnie (Abingdon, UK; NBP1-30209), calprotectin (S100A8/9-HIS) from Cloud-Clone (Hubei, China; RPK504Hu01), and cystatin C (CysC-HIS) from BioVendor (Brno, Czech Republic; RD172009100-H; [Supporting Information Table S-1](#)). Proteins were mixed to form a 4-plex IS with final concentrations of 2.5 μg/mL (CRP-HIS), 3 μg/mL (SAA-HIS), 0.6 μg/mL (S100A8/9-HIS), and 0.6 μg/mL (CysC-HIS).

Reference Samples. Heparin plasma samples were provided by the Institut für Klinische Chemie of the Otto von Guericke University Magdeburg (Magdeburg, Germany). Samples were collected from routine analyses and included normal as well as pathological specimens from patients suffering from acute and chronic inflammation, hematological diseases, kidney disease, gastrointestinal diseases, endocrinological disorders, and other conditions. The studied samples were anonymized after routine analyses. The following methods were used as reference assays: the Tina-quant immuno-turbidimetry assay from Roche/Hitachi (Basel, Switzerland)

for CRP, the ELISA kit MG51951 from IBL (Hamburg, Germany) for SAA, the ELISA kit RD191217100R from BioVendor (Brno, Czech Republic) for S100A8/9, and a nephelometry assay (BN ProSpec) from Siemens (Munich, Germany) for CysC. Reference samples were stored at −80 °C, and all methods were carried out following the manufacturers' protocols. This study is in conformity with the local ethic committee of University of Magdeburg and is of the quality control (QC) category, which according to the current Norwegian regulations is exempt from review by the institutional review board.

Preparation of Antibody-Magnetic Bead Conjugates.

Antibody-magnetic bead conjugates were prepared immediately before use in batches of 450 μL, sufficient for analyses of 96 samples. Conjugation was carried out according to the manufacturers' protocol with minor modifications. Immobilization was performed separately for each antibody, and MBs were mixed in equal volumes before use. A magnetic stand holding 1.5 mL tubes was used throughout the procedure to collect the MBs. Details of the procedure were as follows:

NHS-functionalized magnetic beads in 450 μL of buffer, as provided by the manufacturer, were separated from the buffer and activated by adding 1 mL of ice-cold 1 mM hydrochloric acid. After gently mixing for 15 s, the beads were collected again, and 450 μL of diluted antibody (0.5 mg/mL) was added, followed by incubation for 1.5 h at room temperature under gentle stirring. After conjugation, the MBs were washed twice with 1 mL of 0.1 M glycine and once with 1 mL of ultrapure water to remove excess antibodies. Then, 1 mL of quenching buffer, 3 M ethanolamine (pH 9.0), was immediately added to the collected MBs followed by incubation for 2 h at room temperature under gentle stirring. Finally, after rinsing with 1

mL of ultrapure water and three times with 1 mL of 50 mM borate buffer (pH 8.5), the conjugated beads were stored in borate buffer at 4 °C in aliquots of 450 μ L.

Sample Purification. Serum/plasma samples (20 μ L) were transferred from the plates used for storage into 96-well microtiter plates, then 20 μ L of internal standard was added using a Cybi-Disk robot from CyBio AG (Jena, Germany). Samples were mixed briefly on a shaker. Throughout the procedure, MBs were separated from liquid solutions using the 96-well magnetic plate. Storage buffer was removed from the conjugated MBs and replaced with TBS-T buffer to obtain a bead concentration of 1 mg/mL. Microtiter plates with spiked samples were placed into a Microlab Star Liquid handling station from Hamilton (Stockholm, Sweden), and 10 μ L of the MB suspension was added into each well, followed by aspirating and dispensing the mixture for 1 h (Figure 1). Then, the beads were washed twice with 120 μ L of TBS-T buffer and twice with 120 μ L of pure water to remove nonantigenic proteins and other serum/plasma components. Finally, the captured proteins were eluted from the MBs using 9 μ L of 0.1 M glycine (pH = 2), and the eluents were transferred into a new 96-well plate for MALDI-TOF MS analysis. Analyte enrichment was fully automated, and processing time was 2 h for 384 samples. The failure rate of the automated liquid handling procedure was about 0.4%.

MALDI-TOF MS Analysis. 2,5-DHAP was prepared as a MALDI matrix as described by Wenzel et al.⁶⁸ We modified this protocol with respect to automated sample spotting using the Cybi-Disk robot and a Bruker BigAnchor 384 target plate (Bremen, Germany). Instead of 100% ethanol, we used a mixture of ethanol and acetonitrile (1:3) as a solvent for 2,5-DHAP. Each well containing 9 μ L of eluted sample was filled with 5 μ L of 2,5-DHAP and mixed intensely (Figure 1). A total of 2 μ L of this sample–matrix mixture was dispensed on the BigAnchor 384 target and dried at room temperature. MALDI-TOF MS spectra were acquired by a Bruker UltraFlextreme instrument (Bremen, Germany). Samples were analyzed automatically in positive ion mode with 15 000 laser shots per sample (1 kHz, 500 shots/spot, random pattern), fixed laser intensity (60%), and high-pass filter with a threshold of 5 kDa. The laser beam was rastered randomly over the surface. The time for analyses of 384 samples was 2 h. Spectra were acquired both in linear and reflector ion mode. Acceleration voltage was 25 kV, and detector voltage was 3080 kV in reflector mode and 3400 kV in linear mode. Spectra were smoothed with a Savitzky Golay filter and background subtracted by the Tophat filter using Bruker's flexAnalysis software. Signal intensities were determined from the peak height. Total concentrations of SAA, S100A8/9, and CysC were calculated by summing up the peak heights of the proteoforms, assuming that antigenicities and detection probabilities in MALDI MS were equal for all proteoforms of each marker.

Correction of Mass Interference of S100A9-O₂ and des-S CysC-OH. Signal interference of two proteoforms was corrected prior to quantification. The mass peaks of oxidized S100A9 and des-S CysC-OH differed by 3 Da only and could not be separated by the TOF MS. Running CysC singleplex assays of the ref 80 samples (data not shown) revealed that the sum of des-S CysC + CysC and the sum of des-S CysC-OH + CysC-OH were strongly related ($\rho = 0.98$, $p = 0.001$) with a mean ratio (CV) of 0.88 (12%). Therefore, we adjusted the signal of S100A9-O₂ by estimation and subtraction of the des-S CysC-OH peak height.

Assay Calibration. For quantification of CRP, SAA, S100A8/9, and CysC by MALDI MS, we prepared a standard curve for each marker based on a 4-plex calibrant. Ideally, certified reference materials should be used to prepare the 4-plex calibrant, but this was not feasible in our study because a certified calibrant for S100A8/9 was not available. We tested alternative materials but did not obtain reproducible standard curves using native S100A8/9 extracted from neutrophils or recombinant S100A8/9 (data not shown). However, satisfactory standard curves were obtained by serial dilutions of reference heparin plasma samples. In addition, concentrations of the certified sera of CRP (41.2 μ g/mL) and CysC (5.5 μ g/mL) were too low to cover a sufficiently large concentration range after dilution in a 4-plex assay. Therefore, we prepared an alternative 4-plex calibrant by pooling 13 samples of the heparin plasma samples with high levels of all four markers, and quantified CRP, SAA, and CysC by singleplex assays, calibrated on the certified sera. As a consequence, only a relative method comparison could be performed for S100A8/9. Seven calibrant samples (covering a 256-fold concentration range) were prepared from the pooled reference heparin plasma by serial dilution in TBS (1:1). An additional blank sample of TBS was added as a calibrant. Three replicates were analyzed for each concentration and blank sample.

Assay Characteristics. The limit of detection and quantification (LOD and LOQ) were calculated using the ICH guidelines with $\text{LOD} = 3.3\sigma/s$ and $\text{LOQ} = 10\sigma/s$, where σ was the standard deviation of blank samples (TBS buffer, $N = 16$) and s the slope of the standard curve.⁶⁹

Precision of the method was assessed by calculation of the within-day and between-day variations of the total protein concentrations (sum of all proteoforms) for each marker of three different reference samples. Within-day CVs were determined by analyzing 16 replicates, whereas between-day CVs were determined from three replicates on 10 different days.

A method comparison was performed by passing-Bablok regression and Bland–Altman plots.^{70,71} For Passing-Bablok regression, total concentrations obtained by MALDI-MS were plotted against levels obtained by the reference method. An Excel tool provided by ACOMED statistik (Leipzig, Germany) was used to evaluate correlations in terms of deviations (95% confidence intervals (CIs)) for slope and intercept of the regression line from 1 and 0, respectively.⁷² Bland–Altman plots were prepared by plotting the relative differences between MALDI-TOF MS and the reference methods against the mean levels of both.

RESULTS AND DISCUSSION

Characterization of Mass Spectra. A typical mass spectrum acquired in positive reflector ion mode is shown in Figure 2 spanning a wide mass range from 5 to 24 kDa. Intact complexes of CRP or S100A8/9 were not detected in the higher mass range. Mass signals of the four biomarkers included singly and doubly charged ions, which emerged in the mass spectrum in three patterns at 5–8 kDa, 10–15 kDa, and 22–24 kDa. While the pattern at 5–8 kDa mainly consisted of doubly charged ion species, nearly all proteoforms of the other patterns were singly charged. Signals of antibody fragments or plasma components were weak or absent, demonstrating the high specificity of the immuno-affinity procedure. The signal pattern at 10–15 kDa (inset) included all proteoforms and internal standards and principally allowed the quantification of all

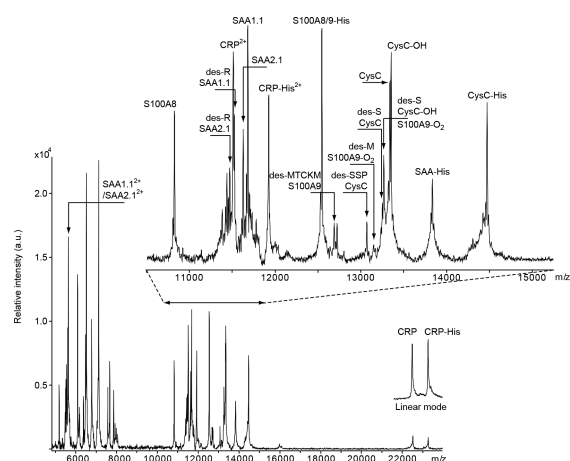


Figure 2. Four-plex immuno-MALDI-TOF MS spectrum of a human plasma sample. Mass spectra of the enriched proteoforms and internal standards were acquired in reflector ion mode and ranged from 5 to 24 kDa. Signals were assigned to three different patterns at 5–8 kDa, 10–15 kDa, and 22–24 kDa. Mass signals between 5 and 8 kDa were doubly charged proteoforms, while the other patterns mainly consisted of singly charged proteoforms with the exception of $(\text{CRP}+2\text{H})^{2+}$. The mass pattern at 10–15 kDa was shown in detail (inset) and included all investigated proteoforms and internal standards (not all SAA truncations were labeled). Due to the mass interference of $(\text{CRP}+2\text{H})^{2+}$ with the truncation des-R SAA1.1, proteoforms of SAA were analyzed by their doubly charged signals (5.6–5.8 kDa), while CRP was quantified by its singly charged species (22–24 kDa). Since the signal-to-noise ratio of $(\text{CRP}+\text{H})^+$ was 4 times higher in linear mode (inset), samples were prepared twice and analyzed in both ion modes to achieve optimal signal quality with respect to resolution and sensitivity.

markers. However, a low mass difference of 3 Da between the singly charged truncation of SAA1.1, lacking an N-terminal arginine amino acid (des-R SAA1.1), and the doubly charged CRP hindered unambiguous quantification of both. Hence, SAA was analyzed by its doubly charged ion species in the mass range of 5.6 to 5.8 kDa, while CRP was quantified using the singly charged signals between 22 and 24 kDa. Since the S/N ratio of $(\text{CRP}+\text{H})^+$ was about 4-times higher in linear than reflector mode (inset), samples were spotted as duplicates on two different target plates and analyzed in both ion modes to achieve maximal resolution and sensitivity for all markers.

Standard Curves. Standard curves were obtained for each marker by plotting the ion signal ratios of the target protein to its IS against the total concentrations (Supporting Information Figure S-1). All curves were nonlinear and could be fitted by polynomial functions of second order with $R^2 > 0.997$. Nonlinear standard curves have been described previously for a similar MALDI assay¹² and may be related to differences in immuno-affinity enrichment or MALDI MS detection between the target protein and the IS.

Assay Performance. Assay precisions for the markers were evaluated in terms of within- and between-day coefficients of variations (CVs, Table 1). Within-day precisions were high and comparable for all four markers, CV ranging from 3.8% to 7.5%. Between-day CVs for CRP, total SAA (tSAA), and total S100A8/9 (tS100A8/9) varied from 7.5% to 9.4%. Between-day CVs of total CysC (tCysC) were similar to within-day CVs and ranged from 3.9% to 5.1%.

Measurement of the four protein biomarkers was sensitive with LODs and LOQs of 0.06 $\mu\text{g}/\text{mL}$ and 0.17 $\mu\text{g}/\text{mL}$ for

Table 1. Within- and Between-Day Variation of Three Different Reference Samples

CRP		tSAA		tS100A8/9		tCysC	
concn ($\mu\text{g}/\text{mL}$)	CV (%)	concn ($\mu\text{g}/\text{mL}$)	CV (%)	concn ($\mu\text{g}/\text{mL}$)	CV (%)	concn ($\mu\text{g}/\text{mL}$)	CV (%)
within-day variation ^a							
5.6	4.9	12.6	4.9	1.7	3.8	1.2	3.9
2.2	4.4	5.3	4.8	1.0	5.0	1.0	5.0
0.7	4.0	1.7	4.5	0.6	7.5	0.9	4.3
between-day variation ^b							
5.6	7.5	12.6	8.6	1.7	8.6	1.2	5.1
2.2	8.2	5.3	9.0	1.0	8.4	1.0	3.9
0.7	9.4	1.7	8.4	0.6	8.7	0.9	4.1

^a $N = 16$. ^b $N = 3 \times 10$ days.

CRP, 0.04 $\mu\text{g}/\text{mL}$ and 0.12 $\mu\text{g}/\text{mL}$ for tSAA, 0.02 $\mu\text{g}/\text{mL}$ and 0.07 $\mu\text{g}/\text{mL}$ for tS100A8/9, and 0.01 $\mu\text{g}/\text{mL}$ and 0.02 $\mu\text{g}/\text{mL}$ for tCysC, respectively.

Compared to other MSIA established for CRP, cystatin C, and SAA, the precision of the present assay was similar or better. In general, assay precision of different MSIA is not related to whether recombinant target proteins or exogenous proteins were used as ISs.^{11,12,73,74} Lower precision compared to our assay has been reported for a method based on the addition of IS to the sample after enrichment,⁷⁵ which underlines the importance of an IS to correct for variations during sample treatment. Detection sensitivity of the method was in the low picomole range and similar to most MSIA. Only an approach for quantification of B-type natriuretic peptide demonstrated lower LODs down to the femtomole range.¹⁸

Biomarker Stability. Protein degradation or denaturation during sample storage and freeze–thaw cycles are crucial for immunoassays. While partial degradation may create artifacts including generation of proteoforms that do not exist in vivo, denaturation can alter antigen–antibody interaction by changing the three-dimensional integrity of the protein. The stabilities of CRP and cystatin C during sample handling and storage have been evaluated in several studies, demonstrating that both proteins in general tolerate several freeze–thaw cycles, and short and long-term storage between +20 °C and –80 °C.^{76–79} Long-term stability data for SAA and S100A8/9 does not exist. While short-term stability data for SAA are not consistent, S100A8/9 has been proven to be stable at +8 °C for 1 week and –20 °C for 6 months.^{80–83} As long as adequate details on stability are not available for these two proteins, sample storage at –80 °C should be mandatory.

Method Comparison. Comparison of our immuno-MALDI MS assay with established techniques showed good between-assay agreement (Figure 3). Signal saturation did not occur for any of the markers within the working ranges, indicating that about 50 μg of antibody per milligram of beads⁸⁴ provided sufficient binding capacity for this four-plex assay.

Good between-assay agreement ($R^2 = 0.963$) was achieved for CRP, covering a wide concentration range of from 0.1 to 100 $\mu\text{g}/\text{mL}$ (Figure 3). The slope (95% CI) obtained by passing-Bablok regression was not different from 1 (0.99, 1.12), while the intercept showed a small but significant deviation (95% CI) of 0.48 $\mu\text{g}/\text{mL}$ (–0.72, –0.26) from 0. Bland–Altman plot confirmed the good between-method agreement by a small average deviation of 2% (Supporting Information Figure S-2).

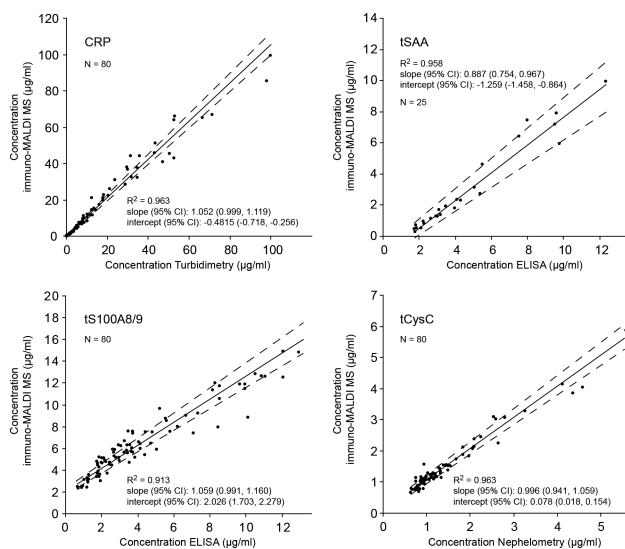


Figure 3. Method comparison between immuno-MALDI-TOF MS and reference techniques using Passing–Bablok regression. Comparison demonstrated linear relationships for all markers with R^2 ranging from 0.963 to 0.913. Best between-assay agreements were obtained for CRP and CysC. Significant difference of the slope from one was obtained for SAA. Significant deviation of the intercept from zero was observed for all markers and was highest for S100A8/9 and SAA. Analyses of SAA were limited to 25 of the 80 reference samples due to saturation of ELISA for values >12 $\mu\text{g}/\text{mL}$.

Validation of SAA was limited to 25 reference samples of tSAA values below 12 $\mu\text{g}/\text{mL}$, because most samples exceeded the analytical range of ELISA. Passing-Bablok comparison demonstrated good linearity ($R^2 = 0.958$), but significant deviations of slope and intercept from 1 (95% CI: (0.75, 0.97)) and 0 (95% CI: (-1.46, -0.86)), respectively (Figure 3). The Bland–Altman plot illustrated the divergence showing higher levels by ELISA than MALDI MS at low tSAA concentrations (Supporting Information Figure S-2).

Total S100A8/9 levels of the reference plasma covered a range from 0.6 to about 13 $\mu\text{g}/\text{mL}$ (Figure 3). When comparing with results based on ELISA assay, we observed good between-assay agreement, but it dropped from $R^2 = 0.941$ to 0.913 after correction for interference with des-S CysC–OH (data not shown). Slope of the regression line did not differ significantly from 1 (95% CI: (0.99, 1.16)), but the intercept showed a significant bias of 2.03 $\mu\text{g}/\text{mL}$ (95% CI: (1.70, 2.28)) from 0. Deviation between the methods decreased with increasing concentration (Supporting Information Figure S-2). Divergence of S100A8/9 levels between immunological assays has been reported previously,^{80,85} and with increasing usage of serum/plasma calprotectin in clinical studies, introduction of certified reference material is crucial for assay harmonization. However, as long as there is no consensus about the exact stoichiometry of the S100A8/9 heterocomplex, immunoassays may differ by capturing uneven portions of different heterocomplexes.

Validation of tCysC, covering plasma levels from 0.63 to 5.58 $\mu\text{g}/\text{mL}$, delivered good linearity ($R^2 = 0.963$) and agreement between immuno-MALDI MS and nephelometry (Figure 3). While the slope did not differ significantly from 1 (95% CI: (0.94, 1.06)), the intercept showed a minor but significant deviation from 0 (95% CI: (0.02, 0.15)). The average deviation

(about 7%) and the limit of agreement (23%) between the two methods were low (Supporting Information Figure S-2).

Quantification of Proteoforms. All proteoforms observed in this work have been described previously by different MS approaches (Supporting Information Table S-1). CRP was detected as mCRP only, most probably derived from dissociation of the native pentameric form during sample preparation. The pro-inflammatory mCRP has been described exclusively in tissues,²⁸ and it is unlikely that mCRP generated in vivo contributed substantially to the levels measured in serum/plasma. Application of a monoclonal antibody against mCRP could clarify its site of origin.⁸⁶

SAA demonstrated large microheterogeneity depending on the expressed genes and truncations (Supporting Information Figure S-3). SAA1 and SAA2 exist as 5 and 2 allelic variants, respectively, which in combination with 2 N-terminal posttranslational truncations, des-R and des-RS, can be expressed as 21 different proteoforms (Supporting Information Table S-1). However, several of the proteoforms had very low abundances and/or overlapped in the mass spectra, limiting the number of detectable proteoforms to 11. SAA1 represented the most prominent proteoforms in the 80 reference samples with a relative abundance of 71% (Supporting Information Figure S-4), while SAA2.1 accounted for 21% only. SAA1.3 and -2.2 were difficult to disentangle by automated peak identification in many samples. Therefore, these proteoforms were analyzed together and contributed on average 8% to tSAA. Visual inspection of the mass signals revealed that SAA1.3 and -2.2 contributed equally to the combined ion signal. Furthermore, the des-R truncations of both isoforms overlapped with the des-RS SAA1.2. The relative proportion of SAA truncations varied strongly between individuals with CVs between 27% and 41% (Supporting Information Figure S-5). Shorter truncations as described by Trenchevska et al.⁷⁴ were not detected in our analyses.

The heterocomplexes of S100A8/9 were detectable by its S100A8 and S100A9 monomers with relative abundances of 74% and 26%, respectively, and consisted of four different proteoforms (Supporting Information Table S-1). Intact complexes of S100A8/9, as described by Vogl et al.,⁴⁹ were not detected by our method. We assume that the majority of the monomers originated from dissociated heterocomplexes, since the amount of circulating monomers has been reported to be minor.⁸⁷ However, the 3 times higher fraction of S100A8 compared to S100A9 was not consistent with any described structure of S100A8/9 heterocomplexes. Between individuals, the proportions of the proteoforms varied with CVs from 6% (S100A8) to 48% (des-M S100A9; Supporting Information Figure S-5).

CysC consisted of five proteoforms (Supporting Information Table S-1), and the obtained relative amounts were consistent with earlier findings.¹² Hydroxylated and native CysC represented the most abundant proteoforms contributing to tCysC with on average 40% and 35%, respectively (Supporting Information Figure S-5). Variation of the relative abundances of proteoforms among individuals was very low for the non-truncated forms with a CV of 5%, while the highest variation was observed for des-SSP CysC with a CV of 26%.

CONCLUSION

This study has described a four-plex immuno-MALDI approach for the targeted quantification of three inflammatory markers, CRP, SAA, and S100A8/9, and the functional marker of kidney

function, CysC. The method allowed sensitive and precise quantification of all four markers, and comparison with established immunoassays demonstrated high agreement for CRP, SAA, and CysC. Lack of certified materials for S100A8/9 allowed relative comparison only, and underlined the urgent demand for harmonization of calprotectin immunoassays. Our method delivered detailed insights into the biomarkers' diversities by identifying up to 20 proteoforms per sample, and especially SAA demonstrated large heterogeneity between individuals. Various immuno-MS approaches have been established for targeted protein quantification. Most of these methods are bottom-up approaches and are based on the positive identification of selected peptides often by Multiple Reaction Monitoring (MRM) mass spectrometry. With the introduction of Stable Isotope Standards and Capture by Anti-Peptide Antibodies (SISCAPA) and immuno-MALDI (iM-ALDI) assays, sensitivities of bottom-up techniques improved dramatically with LODs down to the attomole range.^{88–90} In contrast, direct protein detection by immuno-MALDI-TOF MS covers modifications of the entire protein sequence and is less labor intense, which allows fast investigation of structurally similar proteoforms of multiple biomarkers. Among diverse immuno-affinity formats applied in MS, functionalized superparamagnetic beads have become very popular because of their high versatility and easy workflow.^{17,91,92} However, the application of superparamagnetic beads in top-down approaches is still rare. In this work, we have evaluated commercially available beads, which delivered robust antibody immobilization, low unspecific binding, and high assay capacity. The high-throughput and the low sample consumption make this method well suited for assessment of inflammation and renal status in large cohort studies. The assay is currently used for screening of different biobanks to obtain levels of biomarkers and with-subject reproducibility measures in various healthy and clinical cohorts.

■ ASSOCIATED CONTENT

📄 Supporting Information

The Supporting Information is available free of charge on the ACS Publications website at DOI: 10.1021/acs.analchem.7b04975.

One table with sequences and molecular weights of investigated proteoforms and internal standards; five figures showing standard curves for quantification of CRP, tSAA, tS100A8/9, and tCysC; a method comparison between immuno-MALDI MS and reference methods using Bland Altman tests; mass spectra of SAA proteoforms; relative abundances of SAA proteoforms in 80 human plasma samples; and variability of SAA, S100A8/9, and CysC proteoforms among 80 human plasma samples (PDF).

■ AUTHOR INFORMATION

Corresponding Author

*E-mail: Jie.Gao@uib.no.

ORCID

Jie Gao: 0000-0002-8477-5318

Notes

The authors declare no competing financial interest.

■ REFERENCES

- (1) Anderson, N. L. *Clin. Chem.* **2010**, *56*, 177–185.
- (2) Boschetti, E.; D'Amato, A.; Candiano, G.; Righetti, P. G. *J. Proteomics* **2017**, *17*, 30285–30293.
- (3) Nedelkov, D.; Kiernan, U. A.; Niederkofler, E. E.; Tubbs, K. A.; Nelson, R. W. *Proc. Natl. Acad. Sci. U. S. A.* **2005**, *102*, 10852–10857.
- (4) Walsh, G.; Jefferis, R. *Nat. Biotechnol.* **2006**, *24*, 1241–1252.
- (5) Nelson, R. W.; Krone, J. R.; Bieber, A. L.; Williams, P. *Anal. Chem.* **1995**, *67*, 1153–1158.
- (6) Kiernan, U. A.; Phillips, D. A.; Trenchevska, O.; Nedelkov, D. *PLoS One* **2011**, *6*, e17282.
- (7) Kelleher, N. L.; Lin, H. Y.; Valaskovic, G. A.; Aaserud, D. J.; Fridriksson, E. K.; McLafferty, F. W. *J. Am. Chem. Soc.* **1999**, *121*, 806–812.
- (8) Chait, B. T. *Science* **2006**, *314*, 65–66.
- (9) Kaufmann, R. *J. Biotechnol.* **1995**, *41*, 155–175.
- (10) Cho, Y. T.; Su, H.; Wu, W. J.; Hou, M. F.; Kuo, C. H.; Shiea, J. *Adv. Clin. Chem.* **2015**, *69*, 209–254.
- (11) Trenchevska, O.; Nedelkov, D. *Proteome Sci.* **2011**, *9*, 19–26.
- (12) Meyer, K.; Ueland, P. M. *Anal. Chem.* **2014**, *86*, 5807–5814.
- (13) Patrie, S. M.; Mrksich, M. *Anal. Chem.* **2007**, *79*, 5878–5887.
- (14) Kim, Y. E.; Yi, S. Y.; Lee, C. S.; Jung, Y.; Chung, B. H. *Analyst* **2012**, *137*, 386–392.
- (15) Kiernan, U. A.; Tubbs, K. A.; Gruber, K.; Nedelkov, D.; Niederkofler, E. E.; Williams, P.; Nelson, R. W. *Anal. Biochem.* **2002**, *301*, 49–56.
- (16) Chou, P.-H.; Chen, S.-H.; Liao, H.-K.; Lin, P.-C.; Her, G.-R.; Lai, A. C.-Y.; Chen, J.-H.; Lin, C.-C.; Chen, Y.-J. *Anal. Chem.* **2005**, *77*, 5990–5997.
- (17) Sparbier, K.; Wenzel, T.; Dihazi, H.; Blaschke, S.; Muller, G. A.; Deelder, A.; Flad, T.; Kostrzewa, M. *Proteomics* **2009**, *9*, 1442–1450.
- (18) Suzuki, T.; Israr, M. Z.; Heaney, L. M.; Takaoka, M.; Squire, I. B.; Ng, L. L. *Clin. Chem.* **2017**, *63*, 880–886.
- (19) Krastins, B.; Prakash, A.; Sarracino, D. A.; Nedelkov, D.; Niederkofler, E. E.; Kiernan, U. A.; Nelson, R.; Vogelsang, M. S.; Vadali, G.; Garces, A.; Sutton, J. N.; Peterman, S.; Byram, G.; Darbouret, B.; Perusse, J. R.; Seidah, N. G.; Coulombe, B.; Gobom, J.; Portelius, E.; Pannee, J.; Blennow, K.; Kulasingam, V.; Couchman, L.; Moniz, C.; Lopez, M. F. *Clin. Biochem.* **2013**, *46*, 399–410.
- (20) Tubbs, K. A.; Nedelkov, D.; Nelson, R. W. *Anal. Biochem.* **2001**, *289*, 26–35.
- (21) Brun, V.; Dupuis, A.; Adrait, A.; Marcellin, M.; Thomas, D.; Court, M.; Vandenesch, F.; Garin, J. *Mol. Cell. Proteomics* **2007**, *6*, 2139–2149.
- (22) Wellen, K. E.; Hotamisligil, G. S. *J. Clin. Invest.* **2005**, *115*, 1111–1119.
- (23) Grivennikov, S. I.; Greten, F. R.; Karin, M. *Cell* **2010**, *140*, 883–899.
- (24) Fernandez-Sanchez, A.; Madrigal-Santillan, E.; Bautista, M.; Esquivel-Soto, J.; Morales-Gonzalez, A.; Esquivel-Chirino, C.; Durante-Montiel, L.; Sanchez-Rivera, G.; Valadez-Vega, C.; Morales-Gonzalez, J. A. *Int. J. Mol. Sci.* **2011**, *12*, 3117–3132.
- (25) Franks, A. L.; Slansky, J. E. *Anticancer Res.* **2012**, *32*, 1119–1136.
- (26) Guarner, V.; Rubio-Ruiz, M. E. *Interdiscip. Top. Gerontol.* **2014**, *40*, 99–106.
- (27) Pepys, M. B.; Hirschfield, G. M. *J. Clin. Invest.* **2003**, *111*, 1805–1812.
- (28) Eisenhardt, S. U.; Thiele, J. R.; Bannasch, H.; Stark, G. B.; Peter, K. *Cell Cycle* **2009**, *8*, 3885–3892.
- (29) Ridker, P. M.; Buring, J. E.; Cook, N. R.; Rifai, N. *Circulation* **2003**, *107*, 391–397.
- (30) Kaptoge, S.; Di Angelantonio, E.; Lowe, G.; Pepys, M. B.; Thompson, S. G.; Collins, R.; Danesh, J. *Lancet* **2010**, *375*, 132–140.
- (31) Heikkila, K.; Ebrahim, S.; Lawlor, D. A. *J. Epidemiol. Commun. H* **2007**, *61*, 824–832.
- (32) Eklund, K. K.; Niemi, K.; Kovanen, P. T. *Crit. Rev. Immunol.* **2012**, *32*, 335–348.
- (33) De Buck, M.; Gouwy, M.; Wang, J. M.; Van Snick, J.; Opdenakker, G.; Struyf, S.; Van Damme, J. *Curr. Med. Chem.* **2016**, *23*, 1725–1755.

- (34) Kiernan, U. A.; Tubbs, K. A.; Nedelkov, D.; Niederkofler, E. E.; Nelson, R. W. *FEBS Lett.* **2003**, *537*, 166–170.
- (35) Hua, S.; Song, C.; Geczy, C. L.; Freedman, S. B.; Witting, P. K. *Redox Rep.* **2009**, *14*, 187–196.
- (36) King, V. L.; Thompson, J.; Tannock, L. R. *Curr. Opin. Lipidol.* **2011**, *22*, 302–307.
- (37) Zewinger, S.; Drechsler, C.; Kleber, M. E.; Dressel, A.; Riffel, J.; Triem, S.; Lehmann, M.; Kopecky, C.; Saemann, M. D.; Lepper, P. M.; Silbernagel, G.; Scharnagl, H.; Ritsch, A.; Thorand, B.; de Las Heras Gala, T.; Wagenpfeil, S.; Koenig, W.; Peters, A.; Laufs, U.; Wanner, C.; Fliser, D.; Speer, T.; Marz, W. *Eur. Heart J.* **2015**, *36*, 3007–3016.
- (38) Marhaug, G.; Downton, S. B. *Baillieres Clin Rheumatol* **1994**, *8*, 553–573.
- (39) Hwang, Y. G.; Balasubramani, G. K.; Metes, I. D.; Levesque, M. C.; Bridges, S. L., Jr.; Moreland, L. W. *Arthritis Res. Ther.* **2016**, *18*, 108–116.
- (40) Jylhava, J.; Haarala, A.; Eklund, C.; Pertovaara, M.; Kahonen, M.; Hutri-Kahonen, N.; Levula, M.; Lehtimaki, T.; Huupponen, R.; Jula, A.; Juonala, M.; Viikari, J.; Raitakari, O.; Hurme, M. *J. Intern. Med.* **2009**, *266*, 286–295.
- (41) Malle, E.; Sodin-Semrl, S.; Kovacevic, A. *Cell. Mol. Life Sci.* **2009**, *66*, 9–26.
- (42) Yassine, H. N.; Trenchevska, O.; He, H.; Borges, C. R.; Nedelkov, D.; Mack, W.; Kono, N.; Koska, J.; Reaven, P. D.; Nelson, R. W. *PLoS One* **2015**, *10*, e0115320.
- (43) Rosin, D. L.; Okusa, M. D. *J. Am. Soc. Nephrol.* **2011**, *22*, 416–425.
- (44) Schiopu, A.; Cotoi, O. S. *Mediators Inflammation* **2013**, *2013*, e828354.
- (45) Hessian, P. A.; Fisher, L. *Eur. J. Biochem.* **2001**, *268*, 353–363.
- (46) De Seny, D.; Fillet, M.; Ribbens, C.; Marée, R.; Meuwis, M.-A.; Lutterli, L.; Chapelle, J.-P.; Wehenkel, L.; Louis, E.; Merville, M.-P.; Malaise, M. *Clin. Chem.* **2008**, *54*, 1066–1075.
- (47) Korndorfer, I. P.; Brueckner, F.; Skerra, A. *J. Mol. Biol.* **2007**, *370*, 887–898.
- (48) Vog, T.; Roth, J.; Sorg, C.; Hillenkamp, F.; Strupat, K. *J. Am. Soc. Mass Spectrom.* **1999**, *10*, 1124–1130.
- (49) Vogl, T.; Leukert, N.; Barczyk, K.; Strupat, K.; Roth, J. *Biochim. Biophys. Acta, Mol. Cell Res.* **2006**, *1763*, 1298–1306.
- (50) Van Rheenen, P. F.; Van de Vijver, E.; Fidler, V. *Brit Med. J.* **2010**, *341*, e3369.
- (51) Hammer, H. B.; Odegard, S.; Fagerhol, M. K.; Landewe, R.; van der Heijde, D.; Uhlig, T.; Mowinckel, P.; Kvien, T. K. *Ann. Rheum. Dis.* **2007**, *66*, 1093–1097.
- (52) Larsson, P. T.; Hallerstrom, S.; Rosfors, S.; Wallen, N. H. *Int. Angiol.* **2005**, *24*, 43–51.
- (53) Pedersen, L.; Nybo, M.; Poulsen, M. K.; Henriksen, J. E.; Dahl, J.; Rasmussen, L. M. *BMC Cardiovasc. Disord.* **2014**, *14*, 196–203.
- (54) Ghavami, S.; Chitayat, S.; Hashemi, M.; Eshraghi, M.; Chazin, W. J.; Halayko, A. J.; Kerkhoff, C. *Eur. J. Pharmacol.* **2009**, *625*, 73–83.
- (55) Raimundo, M.; Lopes, J. A. *Cardiol Res. Pract* **2011**, *2011*, 747861.
- (56) Hernandez, S. S. a. G. T. *J. Nephropathol.* **2014**, *3*, 99–104.
- (57) Dharnidharka, V. R.; Kwon, C.; Stevens, G. *Am. J. Kidney Dis.* **2002**, *40*, 221–226.
- (58) Roos, J. F.; Doust, J.; Tett, S. E.; Kirkpatrick, C. M. *Clin. Biochem.* **2007**, *40*, 383–391.
- (59) Uchida, K.; Gotoh, A. *Clin. Chim. Acta* **2002**, *323*, 121–128.
- (60) Koc, M.; Batur, M. K.; Karaarslan, O.; Abali, G. *Cardiol J.* **2010**, *17*, 374–380.
- (61) Angelidis, C.; Deftereos, S.; Giannopoulos, G.; Anatoliotakis, N.; Bouras, G.; Hatzis, G.; Panagopoulou, V.; Pyrgakis, V.; Cleman, M. W. *Curr. Top. Med. Chem.* **2013**, *13*, 164–179.
- (62) Wilson, M. E.; Boumaza, L.; Lacomis, D.; Bowser, R. *PLoS One* **2010**, *5*, e15133.
- (63) Mathews, P. M.; Levy, E. *Ageing Res. Rev.* **2016**, *32*, 38–50.
- (64) Trenchevska, O.; Nedelkov, D. *Proteome Sci.* **2011**, *9*, 19.
- (65) Nedelkov, D.; Shaik, S.; Trenchevska, O.; Aleksovski, V.; Mitrevski, A.; Stojanoski, K. *Open Proteomics J.* **2008**, *1*, 54–58.
- (66) Yassine, H. N.; Trenchevska, O.; Dong, Z.; Bashawri, Y.; Koska, J.; Reaven, P. D.; Nelson, R. W.; Nedelkov, D. *Proteome Sci.* **2016**, *14*, 7–15.
- (67) Trenchevska, O.; Koska, J.; Sinari, S.; Yassine, H.; Reaven, P. D.; Billheimer, D. D.; Nelson, R. W.; Nedelkov, D. *Clinical Mass Spectrometry* **2016**, *1*, 27–31.
- (68) Wenzel, S. K.; Mieruch, T.; Kostrzewa, M.; Spärbier, K. *Rapid Commun. Mass Spectrom.* **2006**, *20*, 785–789.
- (69) Validation of analytical procedures: Text and Methodology. International Conference on Harmonization (ICH) of Technical Requirements for the Registration of Pharmaceuticals for Human Use; Geneva, Switzerland, 1996.
- (70) Passing, H.; Bablok, H. *Clin. Chem. Lab. Med.* **1983**, *21*, 709–720.
- (71) Bland, J. M.; Altman, D. G. *Lancet* **1986**, *327*, 307–310.
- (72) ACOMED statistik: Dienstleister für statistische Planung und Auswertung, Biometrie, Statistik-Beratung für Forschung, Industrie (IVD-Unternehmen) und Universität, Statistik-Schulung. <http://www.acomed-statistik.de/>.
- (73) Kiernan, U. A.; Addobbati, R.; Nedelkov, D.; Nelson, R. W. *J. Proteome Res.* **2006**, *5*, 1682–1687.
- (74) Trenchevska, O.; Yassine, H. N.; Borges, C. R.; Nelson, R. W.; Nedelkov, D. *Biomarkers* **2016**, *21*, 743–751.
- (75) Wang, K.-Y.; Chuang, S.-A.; Lin, P.-C.; Huang, L.-S.; Chen, S.-H.; Ouarda, S.; Pan, W.-H.; Lee, P.-Y.; Lin, C.-C.; Chen, Y.-J. *Anal. Chem.* **2008**, *80*, 6159–6167.
- (76) Aziz, N.; Fahey, J. L.; Detels, R.; Butch, A. W. *Clin. Diagn. Lab. Immunol.* **2003**, *10*, 652–657.
- (77) Erlandsen, E. J.; Randers, E.; Kristensen, J. H. *Scand. J. Clin. Lab. Invest.* **1999**, *59*, 1–8.
- (78) Gislefoss, R. E.; Grimsrud, T. K.; Morkrid, L. *Clin. Chem. Lab. Med.* **2009**, *47*, 596–603.
- (79) Doumatey, A. P.; Zhou, J.; Adeyemo, A.; Rotimi, C. *Clin. Biochem.* **2014**, *47*, 315–318.
- (80) Biovendor. Biovendor Product Brochure, 2014.
- (81) Hillstrom, A.; Tvedten, H.; Lilliehook, I. *Acta Vet. Scand.* **2010**, *52*, 8.
- (82) Ton, H.; Brandsnes, Dale, S.; Holtlund, J.; Skuibina, E.; Schjonsby, H.; John, B. *Clin. Chim. Acta* **2000**, *292*, 41–54.
- (83) Tothova, C.; Nagy, O.; Seidel, H.; Kovac, G. *Vet. Med. Int.* **2012**, *2012*, 861458.
- (84) Thermoscientific User Guide: Pierce NHS-Activated Magnetic Beads, 2013.
- (85) Nilsen, T.; Sunde, K.; Larsson, A. *J. Inflammation* **2015**, *12*, 1–8.
- (86) Schwedler, S. B.; Amann, K.; Wernicke, K.; Krebs, A.; Nauck, M.; Wanner, C.; Potempa, L. A.; Galle, J. *Circulation* **2005**, *112*, 1016–1023.
- (87) Yasar, O.; Akcay, T.; Obek, C.; Turegun, F. A. *Scand. J. Clin. Lab. Invest.* **2017**, *77*, 437–441.
- (88) Weiss, F.; van den Berg, B. H.; Planatscher, H.; Pynn, C. J.; Joos, T. O.; Poetz, O. *Biochim. Biophys. Acta, Proteins Proteomics* **2014**, *1844*, 927–932.
- (89) Anderson, N. L.; Anderson, N. G.; Haines, L. R.; Hardie, D. B.; Olafson, R. W.; Pearson, T. W. *J. Proteome Res.* **2004**, *3*, 235–244.
- (90) Jiang, J.; Parker, C. E.; Hoadley, K. A.; Perou, C. M.; Boysen, G.; Borchers, C. H. *Proteomics: Clin. Appl.* **2007**, *1*, 1651–1659.
- (91) Villanueva, J.; Philip, J.; Entenberg, D.; Chaparro, C. A.; Tanwar, M. K.; Holland, E. C.; Tempst, P. *Anal. Chem.* **2004**, *76*, 1560–1570.
- (92) Peter, J. F.; Otto, A. M. *Proteomics* **2010**, *10*, 628–633.

Supporting information for:

Multiplex immuno-MALDI-TOF MS for
targeted quantification of protein biomarkers and
their proteoforms related to inflammation and
renal dysfunction

Jie Gao*, Klaus Meyer[†], Katrin Borucki[‡], and Per Magne Ueland

Department of Clinical Science, University of Bergen, and Laboratory of Clinical
Biochemistry,
Haukeland University Hospital
5021 Bergen, Norway

[†]Bevital AS
Jonas Lies veg 87, Laboratory building, 9th floor
5021 Bergen, Norway

[‡]Institute for Clinical Chemistry and Pathobiochemistry, Leipziger Strasse 44
Otto-von-Guericke University Magdeburg
39120 Magdeburg, Germany

*Corresponding author
email: Jie.Gao@uib.no

The supporting material includes:

1. Sequences and molecular weights of investigated proteoforms and internal standards.
2. Standard curves for quantification of CRP, tSAA, tS100A8/9 and tCysC.
3. Method comparison between immuno-MALDI-TOF MS and reference methods using Bland Altman tests.
4. Mass spectra of SAA proteoforms.
5. Relative abundances of SAA proteoforms in 80 human plasma samples.
6. Variability of SAA, S100A8/9 and CysC proteoforms among 80 human plasma samples.

Protein	Proteoform	Sequence ^a	Average molecular weight (Da), [Proteoform]	Reference/ Manufacture
CRP	CRP	QTDMSRKAFV FPKESDTSYV SLKAPLTKPL KAFTVCLHFY TELSSTRGYS IFSYATKRQD NEILIFWSKD IGYSFTVGGG EILFEVPEVT VAPVHICTSW ESASGIVEFW VDGKPRVRKS LKKGYTVGAE ASILGQEQD SFGGNFEFSQ SLVGDIGNVN MWDFVLPDE INTIYLGPGF SPNVLNWRAL KYEVQGEVFT KPQLWP	23047.08	Ref. 3, 12, 16
	CRP-HIS	QTDMSRKAFV FPKESDTSYV SLKAPLTKPL KAFTVCLHFY TELSSTRGYS IFSYATKRQD NEILIFWSKD IGYSFTVGGG EILFEVPEVT VAPVHICTSW ESASGIVEFW VDGKPRVRKS LKKGYTVGAE ASILGQEQD SFGGNFEFSQ SLVGDIGNVN MWDFVLPDE INTIYLGPGF SPNVLNWRAL KYEVQGEVFT KPQLWPHHHH HH	23869.93	Arcotec
S100A8/9	S100A8	MLTELEKALN SIIDVYHKYS LIKGNFHAVY RDDLLKLEET ECPQYIRKKG ADVVFKELDI NTDGAVNFQE FLILVIKMGV AAHKSHEES HKE	10834.48	
	S100A9-O ₂	MTCKMSQLER NIETIINTFH QYSVKLGHPD TLNQGEFKEL VRKDLQNFLE KENKNEKVIE HIMEDLDTNA DKQLSFEEFI MLMARLTWAS HEKMHGDEG PGHHHKPGLG EGTP	13273.97 ^b	
	des-MTCKM S100A9	<u>SQLER</u> NIETIINTFH QYSVKLGHPD TLNQGEFKEL VRKDLQNFLE KENKNEKVIE HIMEDLDTNA DKQLSFEEFI MLMARLTWAS HEKMHGDEG PGHHHKPGLG EGTP	12689.19 ^c	Ref. 45, 47
	des-M S100A9	<u>TCKMSQLER</u> NIETIINTFH QYSVKLGHPD TLNQGEFKEL VRKDLQNFLE KENKNEKVIE HIMEDLDTNA DKQLSFEEFI MLMARLTWAS HEKMHGDEG PGHHHKPGLG EGTP	13152.82 ^c	
	S100A8/9- HIS ^d	N.A.	12540, 12718	Cloud-Clone
SAA ^e	SAA1.x	RSFFSFLGEA FDGARDMWRA YSDMREANYI GSDKYFHARG NYDAAKRGPG <u>G</u> <u>V</u> WAAE <u>A</u> ISD ARENIQRFFG <u>H</u> <u>G</u> AEDSLADQ AANEWGRSGK DPNHFRPAGL PEKY	11682.66 [1.1] ^f , 11740.70 [1.2], 11654.61 [1.3] ^g	
	des-R SAA1.x	<u>S</u> FFSFLGEA FDGARDMWRA YSDMREANYI GSDKYFHARG NYDAAKRGPG <u>G</u> <u>V</u> WAAE <u>A</u> ISD ARENIQRFFG <u>H</u> <u>G</u> AEDSLADQ AANEWGRSGK DPNHFRPAGL PEKY	11526.48 [1.1] ^f , 11584.51 [1.2], 11498.42 [1.3] ^g	
	des-RS SAA1.x	<u>S</u> FFSFLGEA FDGARDMWRA YSDMREANYI GSDKYFHARG NYDAAKRGPG <u>G</u> <u>V</u> WAAE <u>A</u> ISD ARENIQRFFG <u>H</u> <u>G</u> AEDSLADQ AANEWGRSGK DPNHFRPAGL PEKY	11439.39 [1.1] ^f , 11497.43 [1.2] ^f , 11411.34 [1.3] ^g	Ref. 3, 33, 41, 73
	SAA2.x	RSFFSFLGEA FDGARDMWRA YSDMREANYI GSDKYFHARG NYDAAKRGPG GAWAAEVISN ARENIQRLTG <u>H</u> <u>G</u> AEDSLADQ AANKWGRSGR DPNHFRPAGL PEKY	11628.66 [2.1], 11647,71 [2.2] ^g	
	des-R SAA2.x	<u>S</u> FFSFLGEA FDGARDMWRA YSDMREANYI GSDKYFHARG NYDAAKRGPG GAWAAEVISN ARENIQRLTG <u>H</u> <u>G</u> AEDSLADQ AANKWGRSGR DPNHFRPAGL PEKY	11472.47 [2.1], 11491.52 [2.2] ^g	
	des-RS SAA2.x	<u>S</u> FFSFLGEA FDGARDMWRA YSDMREANYI GSDKYFHARG NYDAAKRGPG GAWAAEVISN ARENIQRLTG <u>H</u> <u>G</u> AEDSLADQ AANKWGRSGR DPNHFRPAGL PEKY	11385.39 [2.1], 11404.44 [2.2] ^g	
	SAA-HIS	MGSSHHHHHH SGLVPRGSH MRSFFSFLGE AFDGARDMWR AYSDMREANY IGSDKYFHAR GNYDAAKRG GGVWAAE AIS DARENIQRFF GHGAEDSLAD QAANEWGRSG KDPNHFRPAG LPEKY	13977.18	Novus
CysC	CysC /-OH	<u>S</u> PGKPPRLV GGPMDASVEE EGVRRALDFA VGEYNKASND MYHSRALQVV RARKQIVAGV NYFLDVELGR TTCTKTQPNL DNCPFHDQPH LKRKAFCSFQ IYAVPWQGTMTLSKSTCQDA	13347.12, 13363.11 [-OH] ^h	
	des-S CysC /- OH	<u>S</u> PGKPPRLV GGPMDASVEE EGVRRALDFA VGEYNKASND MYHSRALQVV RARKQIVAGV NYFLDVELGR TTCTKTQPNL DNCPFHDQPH LKRKAFCSFQ IYAVPWQGTMTLSKSTCQDA	13260.04, 13276.04 [-OH] ^{b, h}	Ref. 3, 11, 12, 62, 63
	des-SSP CysC	<u>G</u> KPPRLV GGPMDASVEE EGVRRALDFA VGEYNKASND MYHSRALQVV RARKQIVAGV NYFLDVELGR TTCTKTQPNL DNCPFHDQPH LKRKAFCSFQ IYAVPWQGTMTLSKSTCQDA	13075.85	
	CysC-HIS	MKHHHHHHAS SPGKPPRLVG GPMMDASVEE EGVRRALDFAV GEYNKASNDM YHSRALQVVR ARKQIVAGVN YFLDVELGRT TCTKTQPNLD NCPFHDPHL KRKAFCSFQI YAVPWQGTMTLSKSTCQDA	14500.41	Biovendor

^a Modifications of protein sequences are assigned in bold (additional amino acid), in bold and underlined (modified/changed amino acid), or as underlined blanks (missing amino acids).

^b Signals of S100A9-O₂ and des-S CysC-OH overlap with a mass difference of 3 Da.

^c N-terminal amino acid is acetylated.

^d Amino acid sequence was not provided by manufacture. Molecular masses are empirical.

^e Changed amino acids compared to SAA1.1: V→A, A→V, G→D for SAA1.2; V→A for SAA1.3; H→R for SAA2.2.

^f SAA1.1 has the same nominal mass as the low abundant forms SAA1.4 and 1.5, which are not listed.

^g SAA1.3 and SAA2.2 overlap with a mass difference of 7 Da; signals of des-RS SAA1.2 and SAA2.2 overlap with a mass difference of 1 Da.

^h Proline is hydroxylated.

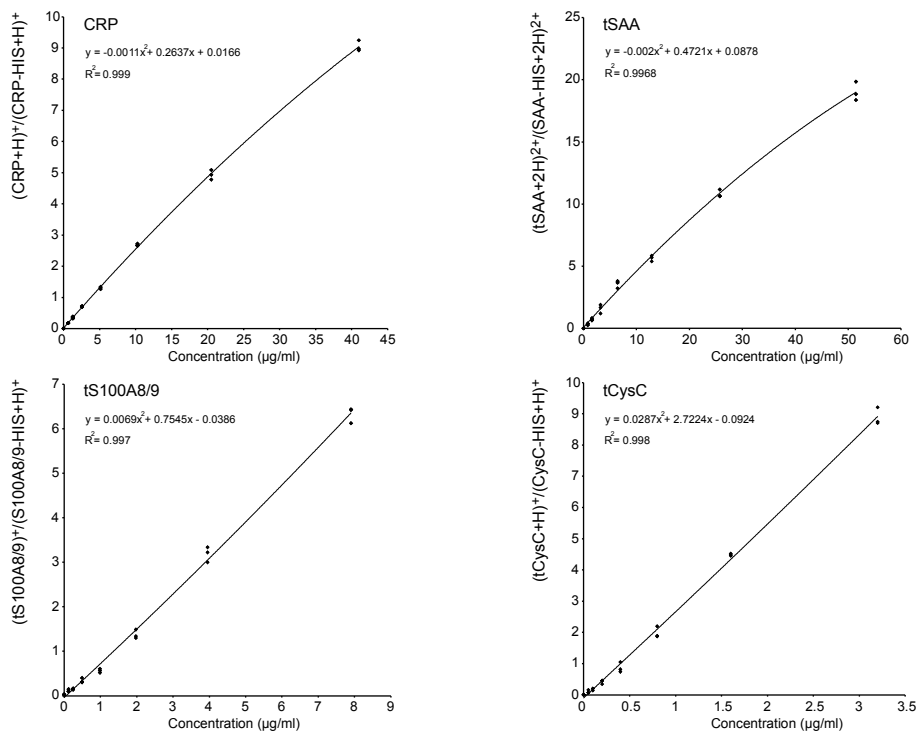


Figure S-1. Standard curves for quantification of CRP, tSAA, tS100A8/9 and tCysC. The signal ratios of the target proteins to their internal standards were plotted against the concentrations of the calibrants. While single charged ion species were used for CRP, tS100A8/9 and tCysC, tSAA was quantified by its doubly charged mass signals. All curves were fitted by polynomial functions of 2nd order with $R^2 > 0.997$.

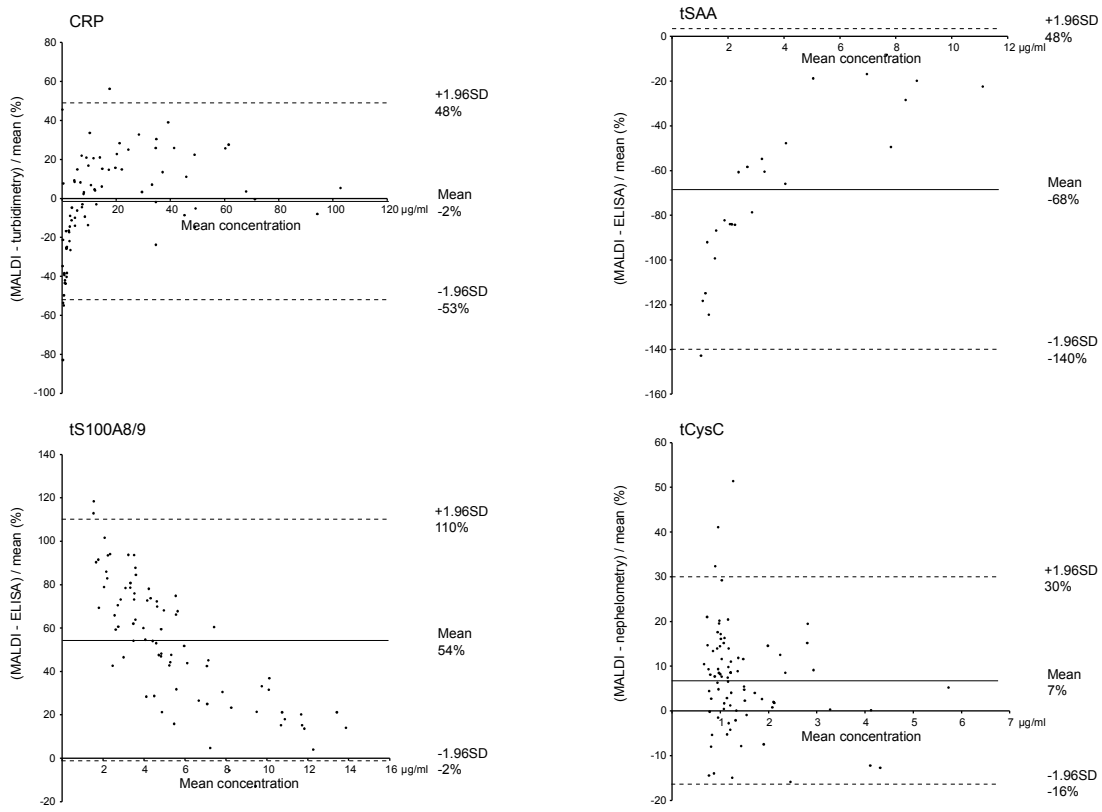


Figure S-2. Method comparison between immuno-MALDI-TOF MS and reference techniques using Bland-Altman tests. The relative differences between immuno-MALDI-TOF MS and reference methods were plotted against their mean concentrations. The overall bias and 95% CI are assigned in the graphs. Bias (%) were low for CRP (-2%) and tCysC (7%), while tSAA (-68%) and tS100A8/9 demonstrated large deviations (54%).

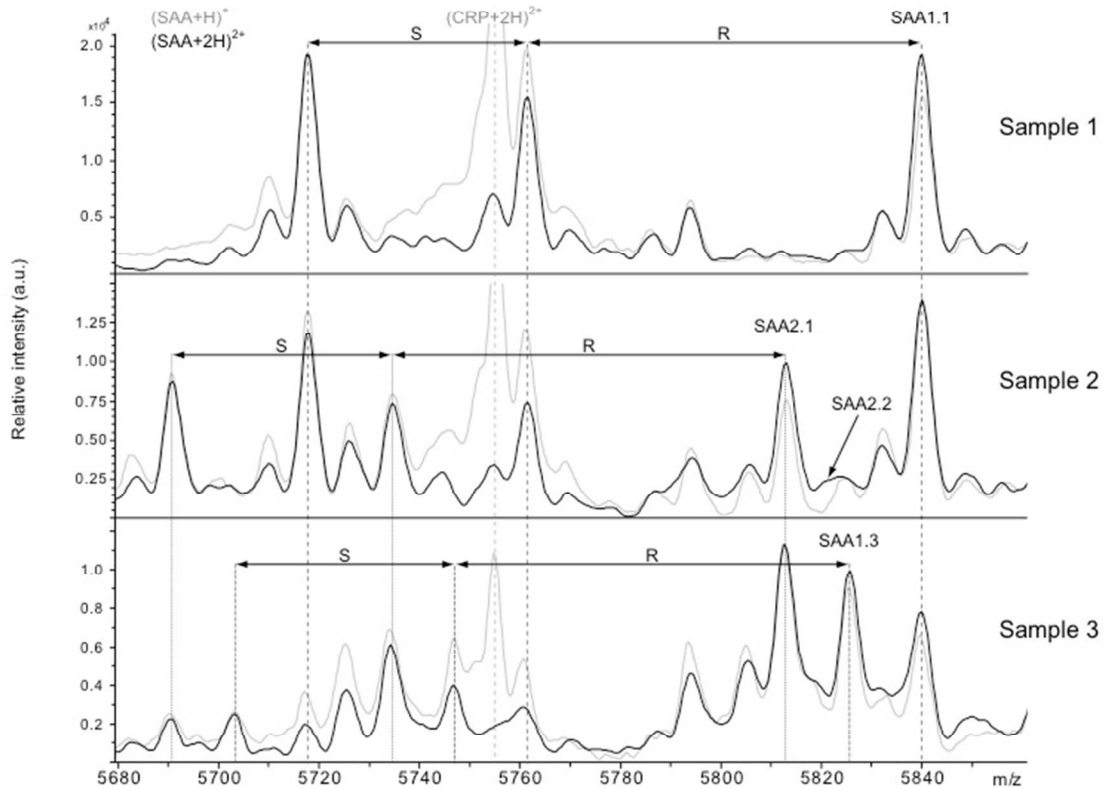
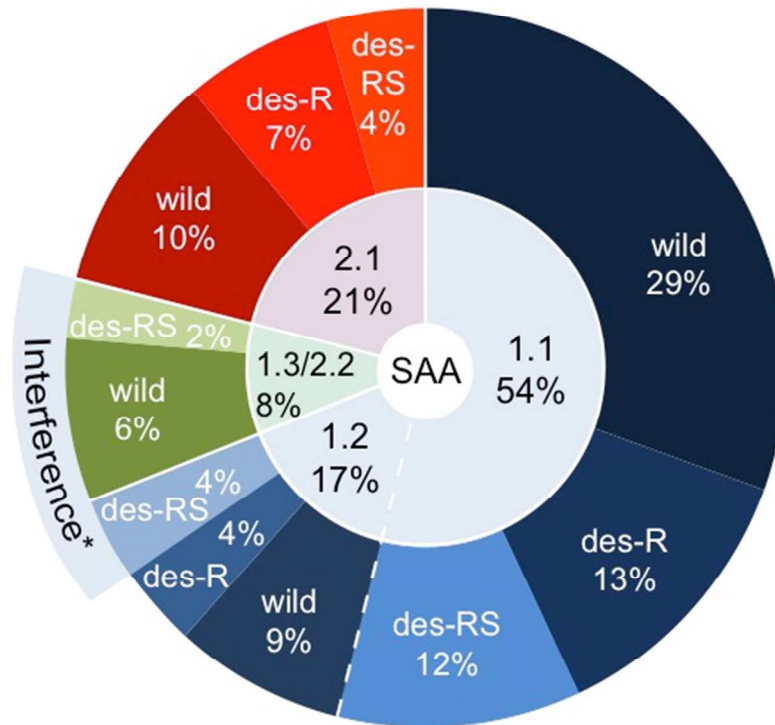


Figure S-3. Mass spectra of SAA proteoforms. Comparison of three different samples demonstrated large variation of SAA proteoforms between subjects related to SAA1 and SAA2 expression and N-terminal truncations lacking an arginine (R) and an arginine-serine dipeptide (RS). Doubly charged mass signals of SAA were used for quantification (spectra in black), since the singly charged signal of des-R SAA1.1 overlapped with the doubly charged signal of CRP (spectra in grey).



* Signal interference of SAA1.2, 1.3 and 2.2 :
 1. SAA 1.3 + SAA2.2
 2. des-RS SAA1.2 + des-R SAA1.3 + des-R SAA2.2

Figure S-4. Relative abundances of SAA1 and SAA2 proteoforms in 80 human plasma samples. SAA1 and SAA2 were obvious as 5 allelic variants (SAA1.1, 1.2, and 1.3; SAA2.1 and 2.2). In addition to 2 posttranslational truncations, des-R and des-RS, up to 11 different proteoforms could be determined. Among them SAA1 and SAA2.1 represented the most abundant proteoforms with relative abundances of 71% and 21%, respectively. Mass signals of SAA1.3, SAA2.2 and des-RS SAA1.2 interfered with each other and were represented with a relative abundance of 12%.

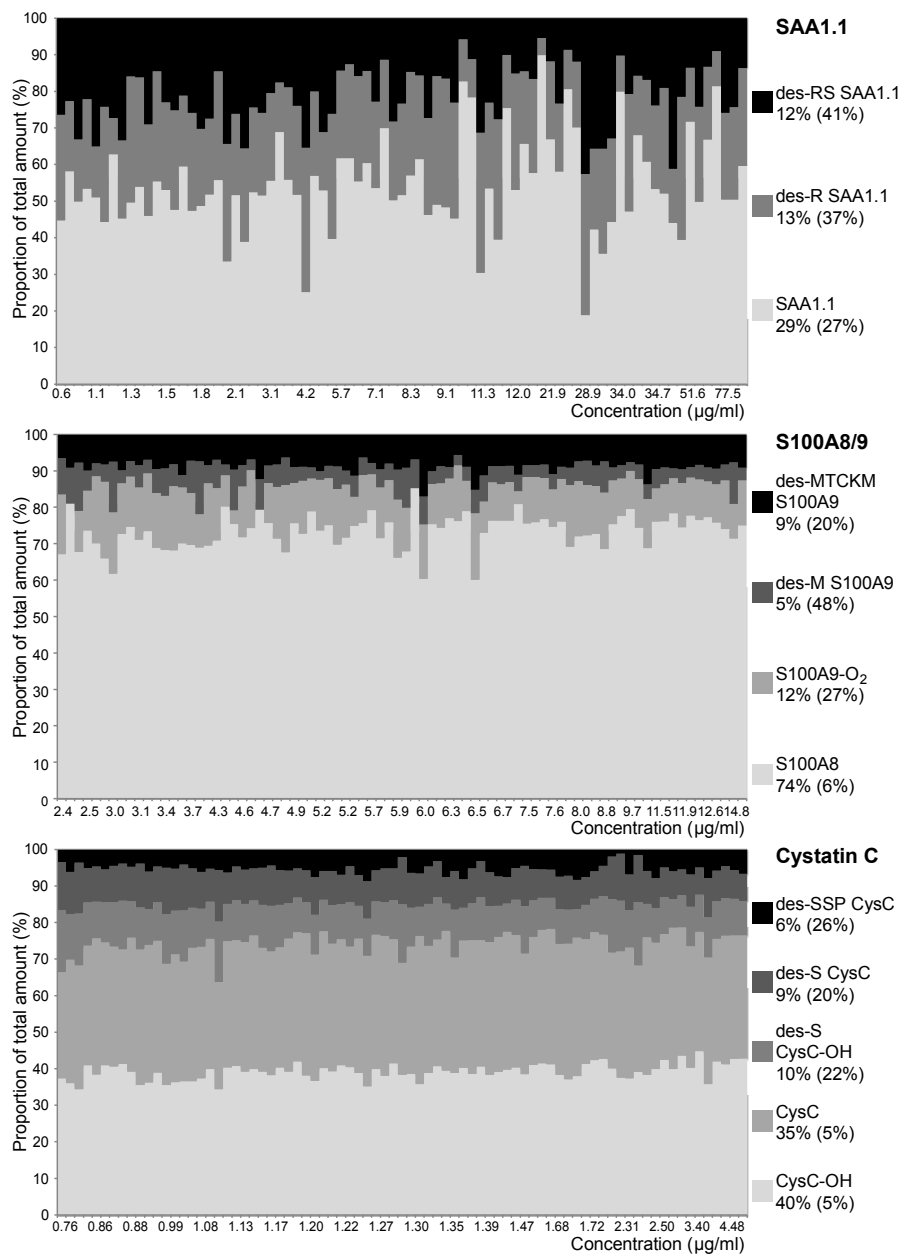


Figure S-5. Variability of SAA1.1, S100A8/9 and CysC proteoforms among 80 human plasma samples. The relative portions of the proteoforms were plotted for all samples and sorted by the total concentrations measured. Proteoforms were labelled by different tones of grey and their relative abundances (CV) were listed. High variations were observed for proteoforms of SAA1.1 with CVs between 27% and 41%, while cystatin C proteoforms varied between 5% and 26%.